PHYSICAL REVIEW C **77**, 011901(R) (2008)

Transverse momentum and centrality dependence of dihadron correlations in Au+Au collisions at $\sqrt{s_{NN}} = 200$ GeV: Jet quenching and the response of partonic matter

A. Adare,[8] S. Afanasiev,[22] C. Aidala,[9] N. N. Ajitanand,[49] Y. Akiba,[43,44] H. Al-Bataineh,[38] J. Alexander,[49] A. Al-Jamel,[38] K. Aoki,[28,43] L. Aphecetche,[51] R. Armendariz,[38] S. H. Aronson,[3] J. Asai,[44] E. T. Atomssa,[29] R. Averbeck,[50] T. C. Awes,[39] B. Azmoun,[3] V. Babintsev,[18] G. Baksay,[14] L. Baksay,[14] A. Baldisseri,[11] K. N. Barish,[4] P. D. Barnes,[31] B. Bassalleck,[37] S. Bathe,[4] S. Batsouli,[9,39] V. Baublis,[42] F. Bauer,[4] A. Bazilevsky,[3] S. Belikov,[3,21,*] R. Bennett,[50] Y. Berdnikov,[46] A. A. Bickley,[8] M. T. Bjorndal,[9] J. G. Boissevain,[31] H. Borel,[11] K. Boyle,[50] M. L. Brooks,[31] D. S. Brown,[38] D. Bucher,[34] H. Buesching,[3] V. Bumazhnov,[18] G. Bunce,[3,44] J. M. Burward-Hoy,[31] S. Butsyk,[31,50] S. Campbell,[50] J.-S. Chai,[23] B. S. Chang,[58] J.-L. Charvet,[11] S. Chernichenko,[18] J. Chiba,[24] C. Y. Chi,[9] M. Chiu,[9,19] I. J. Choi,[58] T. Chujo,[55] P. Chung,[49] A. Churyn,[18] V. Cianciolo,[39] C. R. Cleven,[16] Y. Cobigo,[11] B. A. Cole,[9] M. P. Comets,[40] P. Constantin,[21,31] M. Csanád,[13] T. Csörgő,[25] T. Dahms,[50] K. Das,[15] G. David,[3] M. B. Deaton,[1] K. Dehmelt,[14] H. Delagrange,[51] A. Denisov,[18] D. d'Enterria,[9] A. Deshpande,[44,50] E. J. Desmond,[3] O. Dietzsch,[47] A. Dion,[50] M. Donadelli,[47] J. L. Drachenberg,[1] O. Drapier,[29] A. Drees,[50] A. K. Dubey,[57] A. Durum,[18] V. Dzhordzhadze,[4,52] Y. V. Efremenko,[39] J. Egdemir,[50] F. Ellinghaus,[8] W. S. Emam,[4] A. Enokizono,[17,30] H. En'yo,[43,44] B. Espagnon,[40] S. Esumi,[54] K. O. Eyser,[4] D. E. Fields,[37,44] M. Finger,[5,22] M. Finger Jr.,[5,22] F. Fleuret,[29] S. L. Fokin,[27] B. Forestier,[32] Z. Fraenkel,[57] J. E. Frantz,[9,50] A. Franz,[3] A. D. Frawley,[15] K. Fujiwara,[43] Y. Fukao,[28,43] S.-Y. Fung,[4] T. Fusayasu,[36] S. Gadrat,[32] I. Garishvili,[52] F. Gastineau,[51] M. Germain,[51] A. Glenn,[8,52] H. Gong,[50] M. Gonin,[29] J. Gosset,[11] Y. Goto,[43,44] R. Granier de Cassagnac,[29] N. Grau,[21] S. V. Greene,[55] M. Grosse Perdekamp,[19,44] T. Gunji,[7] H.-Å. Gustafsson,[33] T. Hachiya,[17,43] A. Hadj Henni,[51] C. Haegemann,[37] J. S. Haggerty,[3] M. N. Hagiwara,[1] H. Hamagaki,[7] R. Han,[41] H. Harada,[17] E. P. Hartouni,[30] K. Haruna,[17] M. Harvey,[3] E. Haslum,[33] K. Hasuko,[43] R. Hayano,[7] M. Heffner,[30] T. K. Hemmick,[50] T. Hester,[4] J. M. Heuser,[43] X. He,[16] H. Hiejima,[19] J. C. Hill,[21] R. Hobbs,[37] M. Hohlmann,[14] M. Holmes,[55] W. Holzmann,[49] K. Homma,[17] B. Hong,[26] T. Horaguchi,[43,53] D. Hornback,[52] M. G. Hur,[23] T. Ichihara,[43,44] K. Imai,[28,43] M. Inaba,[54] Y. Inoue,[43,45] D. Isenhower,[1] L. Isenhower,[1] M. Ishihara,[43] T. Isobe,[7] M. Issah,[49] A. Isupov,[22] B. V. Jacak,[50,†] J. Jia,[9] J. Jin,[9] O. Jinnouchi,[44] B. M. Johnson,[3] K. S. Joo,[35] D. Jouan,[40] F. Kajihara,[7,43] S. Kametani,[7,56] N. Kamihara,[43,53] J. Kamin,[50] M. Kaneta,[44] J. H. Kang,[58] H. Kanou,[43,53] T. Kawagishi,[54] D. Kawall,[44] A. V. Kazantsev,[27] S. Kelly,[8] A. Khanzadeev,[42] J. Kikuchi,[56] D. H. Kim,[35] D. J. Kim,[58] E. Kim,[48] Y.-S. Kim,[23] E. Kinney,[8] A. Kiss,[13] E. Kistenev,[3] A. Kiyomichi,[43] J. Klay,[30] C. Klein-Boesing,[34] L. Kochenda,[42] V. Kochetkov,[18] B. Komkov,[42] M. Konno,[54] D. Kotchetkov,[4] A. Kozlov,[57] A. Král,[10] A. Kravitz,[9] P. J. Kroon,[3] J. Kubart,[5,20] G. J. Kunde,[31] N. Kurihara,[7] K. Kurita,[43,45] M. J. Kweon,[26] Y. Kwon,[52,58] G. S. Kyle,[38] R. Lacey,[49] Y.-S. Lai,[9] J. G. Lajoie,[21] A. Lebedev,[21] Y. Le Bornec,[40] S. Leckey,[50] D. M. Lee,[31] M. K. Lee,[58] T. Lee,[48] M. J. Leitch,[31] M. A. L. Leite,[47] B. Lenzi,[47] H. Lim,[48] T. Liška,[10] A. Litvinenko,[22] M. X. Liu,[31] X. Li,[6] X. H. Li,[4] B. Love,[55] D. Lynch,[3] C. F. Maguire,[55] Y. I. Makdisi,[3] A. Malakhov,[22] M. D. Malik,[37] V. I. Manko,[27] Y. Mao,[41,43] L. Mašek,[5,20] H. Masui,[54] F. Matathias,[9,50] M. C. McCain,[19] M. McCumber,[50] P. L. McGaughey,[31] Y. Miake,[54] P. Mikeš,[5,20] K. Miki,[54] T. E. Miller,[55] A. Milov,[50] S. Mioduszewski,[3] G. C. Mishra,[16] M. Mishra,[2] J. T. Mitchell,[3] M. Mitrovski,[49] A. Morreale,[4] D. P. Morrison,[3] J. M. Moss,[31] T. V. Moukhanova,[27] D. Mukhopadhyay,[55] J. Murata,[43,45] S. Nagamiya,[24] Y. Nagata,[54] J. L. Nagle,[8] M. Naglis,[57] I. Nakagawa,[43,44] Y. Nakamiya,[17] T. Nakamura,[17] K. Nakano,[43,53] J. Newby,[30] M. Nguyen,[50] B. E. Norman,[31] A. S. Nyanin,[27] J. Nystrand,[33] E. O'Brien,[3] S. X. Oda,[7] C. A. Ogilvie,[21] H. Ohnishi,[43] I. D. Ojha,[55] H. Okada,[28,43] K. Okada,[44] M. Oka,[54] O. O. Omiwade,[1] A. Oskarsson,[33] I. Otterlund,[33] M. Ouchida,[17] K. Ozawa,[7] R. Pak,[3] D. Pal,[55] A. P. T. Palounek,[31] V. Pantuev,[50] V. Papavassiliou,[38] J. Park,[48] W. J. Park,[26] S. F. Pate,[38] H. Pei,[21] J.-C. Peng,[19] H. Pereira,[11] V. Peresedov,[22] D. Yu. Peressounko,[27] C. Pinkenburg,[3] R. P. Pisani,[3] M. L. Purschke,[3] A. K. Purwar,[31,50] H. Qu,[16] J. Rak,[21,37] A. Rakotozafindrabe,[29] I. Ravinovich,[57] K. F. Read,[39,52] S. Rembeczki,[14] M. Reuter,[50] K. Reygers,[34] V. Riabov,[42] Y. Riabov,[42] G. Roche,[32] A. Romana,[29,*] M. Rosati,[21] S. S. E. Rosendahl,[33] P. Rosnet,[32] P. Rukoyatkin,[22] V. L. Rykov,[43] S. S. Ryu,[58] B. Sahlmueller,[34] N. Saito,[28,43,44] T. Sakaguchi,[3,7,56] S. Sakai,[54] H. Sakata,[17] V. Samsonov,[42] H. D. Sato,[28,43] S. Sato,[3,24,54] S. Sawada,[24] J. Seele,[8] R. Seidl,[19] V. Semenov,[18] R. Seto,[4] D. Sharma,[57] T. K. Shea,[3] I. Shein,[18] A. Shevel,[42,49] T.-A. Shibata,[43,53] K. Shigaki,[17] M. Shimomura,[54] T. Shohjoh,[54] K. Shoji,[28,43] A. Sickles,[50] C. L. Silva,[47] D. Silvermyr,[39] C. Silvestre,[11] K. S. Sim,[26] C. P. Singh,[2] V. Singh,[2] S. Skutnik,[21] M. Slunečka,[5,22] W. C. Smith,[1] A. Soldatov,[18] R. A. Soltz,[30] W. E. Sondheim,[31] S. P. Sorensen,[52] I. V. Sourikova,[3] F. Staley,[11] P. W. Stankus,[39] E. Stenlund,[33] M. Stepanov,[38] A. Ster,[25] S. P. Stoll,[3] T. Sugitate,[17] C. Suire,[40] J. P. Sullivan,[31] J. Sziklai,[25] T. Tabaru,[44] S. Takagi,[54] E. M. Takagui,[47] A. Taketani,[43,44] K. H. Tanaka,[24] Y. Tanaka,[36] K. Tanida,[43,44] M. J. Tannenbaum,[3] A. Taranenko,[49] P. Tarján,[12] T. L. Thomas,[37] M. Togawa,[28,43] A. Toia,[50] J. Tojo,[43] L. Tomášek,[20] H. Torii,[43] R. S. Towell,[1] V.-N. Tram,[29] I. Tserruya,[57] Y. Tsuchimoto,[17,43] S. K. Tuli,[2] H. Tydesjö,[33] N. Tyurin,[18] C. Vale,[21] H. Valle,[55] H. W. van Hecke,[31] J. Velkovska,[55] R. Vertesi,[12] A. A. Vinogradov,[27] M. Virius,[10] V. Vrba,[20] E. Vznuzdaev,[42] M. Wagner,[28,43] D. Walker,[50] X. R. Wang,[38] Y. Watanabe,[43,44] J. Wessels,[34] S. N. White,[3] N. Willis,[40] D. Winter,[9] C. L. Woody,[3] M. Wysocki,[8] W. Xie,[4,44] Y. L. Yamaguchi,[56] A. Yanovich,[18] Z. Yasin,[4] J. Ying,[16] S. Yokkaichi,[43,44] G. R. Young,[39] I. Younus,[37] I. E. Yushmanov,[27] W. A. Zajc,[9] O. Zaudtke,[34] C. Zhang,[9,39] S. Zhou,[6] J. Zimányi,[25,*] and L. Zolin[22]

(PHENIX Collaboration)

[1]*Abilene Christian University, Abilene, Texas 79699, USA*

[2]*Department of Physics, Banaras Hindu University, Varanasi 221005, India*

[3]*Brookhaven National Laboratory, Upton, New York 11973-5000, USA*

[4]*University of California–Riverside, Riverside, California 92521, USA*
[5]*Charles University, Ovocný trh 5, Praha 1, 116 36 Prague, Czech Republic*
[6]*China Institute of Atomic Energy (CIAE), Beijing, People's Republic of China*
[7]*Center for Nuclear Study, Graduate School of Science, University of Tokyo, 7-3-1 Hongo, Bunkyo, Tokyo 113-0033, Japan*
[8]*University of Colorado, Boulder, Colorado 80309, USA*
[9]*Columbia University, New York, New York 10027 and Nevis Laboratories, Irvington, New York 10533, USA*
[10]*Czech Technical University, Zikova 4, 166 36 Prague 6, Czech Republic*
[11]*Dapnia, CEA Saclay, F-91191, Gif-sur-Yvette, France*
[12]*Debrecen University, H-4010 Debrecen, Egyetem tér 1, Hungary*
[13]*ELTE, Eötvös Loránd University, H-1117 Budapest, Pázmány P. s. 1/A, Hungary*
[14]*Florida Institute of Technology, Melbourne, Florida 32901, USA*
[15]*Florida State University, Tallahassee, Florida 32306, USA*
[16]*Georgia State University, Atlanta, Georgia 30303, USA*
[17]*Hiroshima University, Kagamiyama, Higashi-Hiroshima 739-8526, Japan*
[18]*IHEP Protvino, State Research Center of Russian Federation, Institute for High Energy Physics, Protvino RU-142281, Russia*
[19]*University of Illinois at Urbana-Champaign, Urbana, Illinois 61801, USA*
[20]*Institute of Physics, Academy of Sciences of the Czech Republic, Na Slovance 2, 182 21 Prague 8, Czech Republic*
[21]*Iowa State University, Ames, Iowa 50011, USA*
[22]*Joint Institute for Nuclear Research, Moscow Region, RU-141980 Dubna, Russia*
[23]*KAERI, Cyclotron Application Laboratory, Seoul, Korea*
[24]*KEK, High Energy Accelerator Research Organization, Tsukuba, Ibaraki 305-0801, Japan*
[25]*KFKI Research Institute for Particle and Nuclear Physics of the Hungarian Academy of Sciences (MTA KFKI RMKI), H-1525 Budapest 114, P. O. Box 49, Budapest, Hungary*
[26]*Korea University, Seoul 136-701, Korea*
[27]*Russian Research Center "Kurchatov Institute," Moscow, Russia*
[28]*Kyoto University, Kyoto 606-8502, Japan*
[29]*Laboratoire Leprince-Ringuet, Ecole Polytechnique, CNRS-IN2P3, Route de Saclay, F-91128 Palaiseau, France*
[30]*Lawrence Livermore National Laboratory, Livermore, California 94550, USA*
[31]*Los Alamos National Laboratory, Los Alamos, New Mexico 87545, USA*
[32]*LPC, Université Blaise Pascal, CNRS-IN2P3, Clermont-Fd, F-63177 Aubiere Cedex, France*
[33]*Department of Physics, Lund University, Box 118, SE-221 00 Lund, Sweden*
[34]*Institut für Kernphysik, University of Muenster, D-48149 Muenster, Germany*
[35]*Myongji University, Yongin, Kyonggido 449-728, Korea*
[36]*Nagasaki Institute of Applied Science, Nagasaki-shi, Nagasaki 851-0193, Japan*
[37]*University of New Mexico, Albuquerque, New Mexico 87131, USA*
[38]*New Mexico State University, Las Cruces, New Mexico 88003, USA*
[39]*Oak Ridge National Laboratory, Oak Ridge, Tennessee 37831, USA*
[40]*IPN-Orsay, Universite Paris Sud, CNRS-IN2P3, BP1, F-91406 Orsay, France*
[41]*Peking University, Beijing, People's Republic of China*
[42]*PNPI, Petersburg Nuclear Physics Institute, Gatchina, Leningrad Region RU-188300, Russia*
[43]*RIKEN, The Institute of Physical and Chemical Research, Wako, Saitama 351-0198, Japan*
[44]*RIKEN BNL Research Center, Brookhaven National Laboratory, Upton, New York 11973-5000, USA*
[45]*Physics Department, Rikkyo University, 3-34-1 Nishi-Ikebukuro, Toshima, Tokyo 171-8501, Japan*
[46]*Saint Petersburg State Polytechnic University, Saint Petersburg, Russia*
[47]*Universidade de São Paulo, Instituto de Física, Caixa Postal 66318, São Paulo CEP05315-970, Brazil*
[48]*System Electronics Laboratory, Seoul National University, Seoul, Korea*
[49]*Chemistry Department, Stony Brook University, SUNY, Stony Brook, New York 11794-3400, USA*
[50]*Department of Physics and Astronomy, Stony Brook University, SUNY, Stony Brook, New York 11794, USA*
[51]*SUBATECH (Ecole des Mines de Nantes, CNRS-IN2P3, Université de Nantes), BP 20722-44307, Nantes, France*
[52]*University of Tennessee, Knoxville, Tennessee 37996, USA*
[53]*Department of Physics, Tokyo Institute of Technology, Oh-okayama, Meguro, Tokyo 152-8551, Japan*
[54]*Institute of Physics, University of Tsukuba, Tsukuba, Ibaraki 305, Japan*
[55]*Vanderbilt University, Nashville, Tennessee 37235, USA*
[56]*Waseda University, Advanced Research Institute for Science and Engineering, 17 Kikui-cho, Shinjuku-ku, Tokyo 162-0044, Japan*
[57]*Weizmann Institute, Rehovot 76100, Israel*
[58]*Yonsei University, IPAP, Seoul 120-749, Korea*
(Received 22 May 2007; published 7 January 2008)

Azimuthal angle ($\Delta\phi$) correlations are presented for charged hadrons from dijets for $0.4 < p_T < 10$ GeV/c in Au+Au collisions at $\sqrt{s_{\rm NN}} = 200$ GeV. With increasing p_T, the away-side distribution evolves from a broad and relatively flat shape to a concave shape, then to a convex shape. Comparisons to $p+p$ data suggest that the away-side can be divided into a partially suppressed "head" region centered at $\Delta\phi \sim \pi$ and an enhanced "shoulder" region centered at $\Delta\phi \sim \pi \pm 1.1$. The p_T spectrum for the head region softens toward central collisions, consistent with the onset of jet quenching. The spectral slope for the shoulder region is independent of centrality and trigger p_T, which offers constraints on energy transport mechanisms and suggests that it contains the medium response to energetic jets.

DOI: 10.1103/PhysRevC.77.011901 PACS number(s): 25.75.Dw

High transverse momentum (p_T) partons are valuable probes of the high energy density matter created at the Relativistic Heavy-Ion Collider (RHIC). These partons lose a large fraction of their energy in the matter prior to forming hadrons, a phenomenon known as jet quenching. Such energy loss is predicted to lead to strong suppression of both single and correlated away-side dihadron yields at high p_T [1], consistent with experimental findings [2,3]. The exact mechanism for energy loss is not yet understood. Recent results of dihadron azimuthal angle ($\Delta\phi$) correlations have indicated strong modification of the away-side jet [3–6]. For high p_T hadron pairs, such modification is manifested by a partially suppressed away-side peak at $\Delta\phi \sim \pi$ [3]. This has been interpreted as evidence for the fragmentation of jets that survive their passage through the medium.

For intermediate p_T charged hadron pairs, the away-side jet was observed to peak at $\Delta\phi \sim \pi \pm 1.1$ [4,5], suggesting that the energy lost by high p_T partons is transported to lower p_T hadrons at angles away from $\Delta\phi \sim \pi$. The mechanisms for such energy transport include medium deflection of hard [7] or shower partons [8], large-angle gluon radiation [9], Cherenkov gluon radiation [10], and mach-shock medium excitations [11].

In this brief report we present a detailed "mapping" of the p_T and centrality dependence of away-side jet shapes and yields. These measurements allow a detailed investigation of the jet distributions centered around $\Delta\phi \sim \pi \pm 1.1$ and $\Delta\phi \sim \pi$, provide new insight on the interplay between jet quenching and the response of the medium to the lost energy, and provide new constraints for distinguishing the competing mechanisms for energy transport.

The results presented here are based on minimum-bias (MB) Au+Au and $p+p$ datasets as well as a photon level-1 triggered (PT) $p+p$ dataset collected with the PHENIX detector [12] at $\sqrt{s_{\rm NN}} = 200$ GeV, during the 2004–2005 RHIC run. The PT trigger requires a minimum energy of 1.4 GeV in 4×4 electromagnetic calorimeter (EMC) towers in coincidence with the Beam Beam Counters (BBC) [13]. The event centrality was determined via the method in Ref. [12]. A total of 840 million Au+Au events in the vertex range $|z| < 30$ cm was analyzed. Charged particles were reconstructed in the two central arms of PHENIX, each covering -0.35 to 0.35 in pseudorapidity and 90° in azimuth. The tracking system consisted of the drift chambers and two layers of multiwire proportional chambers with pad readout (PC1 and PC3), achieving a momentum resolution of $0.7\% \bigoplus 1.0\%\ p$ (GeV/c) [2].

Dihadron $\Delta\phi$ correlations were obtained by correlating trigger (type A) hadrons with partner (type B) hadrons. The MB and PT $p+p$ datasets were used for trigger $p_T < 5$GeV/c and $p_T > 5$ GeV/c, respectively. To reduce background from decays and conversions, tracks were required to have a matching hit within a $\pm 2.3\sigma$ window in PC3. For $p_T > 4$GeV/c, an additional matching hit at the EMC was required. For triggers with $p_T > 5$ GeV/c, a p_T dependent energy cut in the EMC and a tight $\pm 1.5\sigma$ matching cut at the PC3 were applied to reduce the background to <10% [14]. This energy cut greatly reduces PT trigger bias effects. The PT $p+p$ results are consistent with the MB $p+p$ data for trigger $p_T > 5$ GeV/c.

The jet associated partner yield per trigger, $Y_{\rm jet}(\Delta\phi)$, is obtained by assuming independent contributions from jets and elliptic flow to the $\Delta\phi$ distribution as [4,14]

$$Y_{\rm jet} = \left[\frac{N^s(\Delta\phi)}{N^m(\Delta\phi)} - b_0\left(1 + 2v_2^A v_2^B \cos 2\Delta\phi\right)\right] \times \frac{\int d\Delta\phi N^m(\Delta\phi)}{2\pi N_A \varepsilon_B}, \quad (1)$$

where N_A is the number of triggers, ε_B is the single-particle efficiency for partners in the full azimuth and $|\eta| < 0.35$; $N^s(\Delta\phi)$ and $N^m(\Delta\phi)$ are pair distributions from the same- and mixed-events, respectively. Mixed-event pairs are obtained by selecting partners from different events with similar centrality and vertex. The ε_B values include detector acceptance and reconstruction efficiency, with an uncertainty of ~10% [2,15]. The harmonic term, $2v_2^A v_2^B \cos 2\Delta\phi$, reflects the elliptic flow modulation of the combinatoric pairs in Au+Au [4], where we have assumed $\langle v_2^A v_2^B\rangle$ is factorizable. v_2^A and v_2^B are measured via the reaction plane method [16] using BBC at $3 < |\eta| < 4$. The large rapidity gap between the BBC and the central arm reduces the nonflow contributions, especially those from dijets [17]. The systematic errors on v_2 are estimated to be ~6% for central and midcentral collisions and ~10% for the peripheral collisions [4].

To fix the value of b_0, we followed the subtraction procedure of Refs. [4] and [18] and assumed that $Y_{\rm jet}$ has zero yield at its minimum $\Delta\phi_{\rm min}$ (ZYAM). To estimate the possible oversubtraction at $\Delta\phi_{\rm min}$, we calculate b_0 values independently by fitting $Y_{\rm jet}(\Delta\phi)$ to a function consisting of one near-side and two symmetric away-side Gaussians. The fitting procedure is similar to that used in Ref. [5], except that $|\Delta\phi - \pi| < 1$ is

*Deceased
†PHENIX Spokesperson: jacak@skipper.physics.sunysb.edu

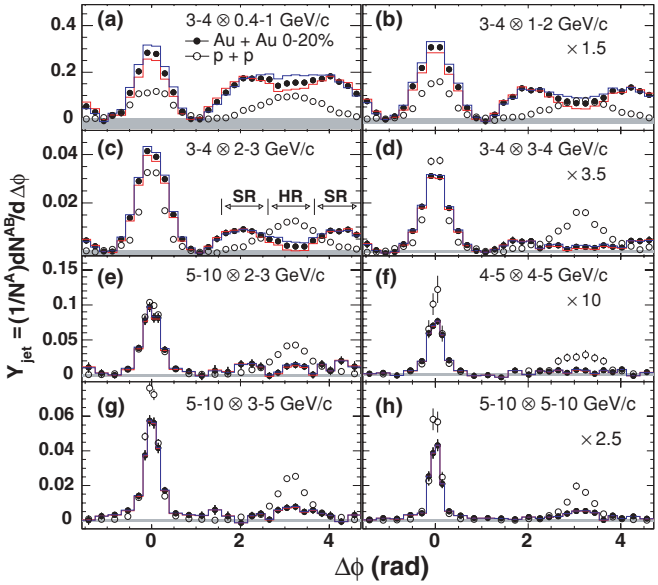

FIG. 1. (Color online) Per-trigger yield versus $\Delta\phi$ for various trigger and partner p_T ($p_T^A \otimes p_T^B$), arranged by increasing pair momentum ($p_T^A + p_T^B$), in $p+p$ and 0–20% Au+Au collisions. The data in some panels are scaled as indicated. Solid histograms (shaded bands) indicate elliptic flow (ZYAM) uncertainties. Arrows in Panel (c) indicate "head" (HR) and "shoulder" (SR) regions. The difference in near-side yield between Au+Au and $p+p$ for Panels (d)–(h) is within the 14% combined uncertainty of the single-particle efficiency.

excluded to avoid punch-through jets around π (see Fig. 1). This fit accounts for the overlap of the near- and away-side Gaussians at $\Delta\phi_{\rm min}$ and thus gives b_0 values systematically lower than that for ZYAM. We assign the differences as one-sided systematic errors on b_0. This oversubtraction error is only significant in central collisions and at $p_{\rm T}^{A,B} < 3$ GeV/c.

The per-trigger yield distributions for $p+p$ and 0–20% central Au+Au collisions are compared in Fig. 1 for various combinations of trigger and partner p_T ranges ($p_T^A \otimes p_T^B$) as indicated. The $p+p$ data show essentially Gaussian away-side peaks centered at $\Delta\phi \sim \pi$ for all p_T^A and p_T^B. In contrast, the Au+Au data show substantial shape modifications dependent on p_T^A and p_T. For a fixed value of p_T^A, Figs. 1(a)–1(d) reveal a striking evolution from a broad, roughly flat peak to a local minimum at $\Delta\phi \sim \pi$ with side peaks at $\Delta\phi \sim \pi \pm 1.1$. Interestingly, the location of the side peaks in $\Delta\phi$ is roughly constant with increasing p_T^B (see also Ref. [5]). Such p_T independence is compatible with the away-side jet modification expected from a medium-induced mach-shock [11] but disfavors models that incorporate large angle gluon radiation [9], Cherenkov gluon radiation [10], or deflected jets [7,8].

For relatively high values of $p_T^A \otimes p_T^B$, Figs. 1(e)–1(h) show that the away-side jet shape for Au+Au gradually becomes peaked as for $p+p$, albeit suppressed. This "reappearance" of the away-side peak seems due to a reduction of the yield centered at $\Delta\phi \sim \pi \pm 1.1$ relative to that at $\Delta\phi \sim \pi$, rather than to a merging of the peaks centered at $\Delta\phi \sim \pi \pm 1.1$. This is consistent with the dominance of dijet fragmentation at large $p_T^A \otimes p_T^B$, possibly due to jets that punch-through the medium [19] or to those emitted tangentially to the medium's surface [20].

The evolution of the away-side jet shape with p_T! (cf. Fig. 1) suggests separate contributions from a medium-induced component centered at $\Delta\phi \sim \pi \pm 1.1$ and a fragmentation component centered at $\Delta\phi \sim \pi$. A model independent study of these contributions can be made by dividing the away-side jet function into equal-sized head ($|\Delta\phi - \pi| < \pi/6$, HR) and shoulder ($\pi/6 < |\Delta\phi - \pi| < \pi/2$, SR) regions, as indicated in Fig. 1(c). We characterize the relative amplitude of these two regions with the ratio, $R_{\rm HS} = \frac{\int_{\Delta\phi\in{\rm HR}} d\Delta\phi Y_{\rm jet}(\Delta\phi)}{\int_{\Delta\phi\in{\rm HR}} d\Delta\phi} / \frac{\int_{\Delta\phi\in{\rm SR}} d\Delta\phi Y_{\rm jet}(\Delta\phi)}{\int_{\Delta\phi\in{\rm SR}} d\Delta\phi}$. Because $N_{\rm A}$ in Eq. (1) cancels in the ratio, $R_{\rm HS}$ is a pure pair variable and is symmetric *w.r.t.* p_T^A and p_T^B: $R_{\rm HS}(p_T^A, p_T^B) = R_{\rm HS}(p_T^B, p_T^A)$. For concave and convex shapes, one expects $R_{\rm HS} < 1$ and $R_{\rm HS} > 1$, respectively.

Figure 2 summarizes the p_T^B dependence of $R_{\rm HS}$ for both $p+p$ and central Au+Au collisions in four p_T^A bins. The ratios for $p+p$ are always above one and increase with p_T^B. This reflects the narrowing of a peaked jet shape with increasing p_T^B [14]. In contrast, the ratios for Au+Au show a nonmonotonic dependence on $p_T^{A,B}$. They evolve from $R_{\rm HS} \sim 1$ for $p_T^{A,B} \lesssim 1$ GeV/c through $R_{\rm HS} < 1$ for $1 \lesssim p_T^{A,B} \lesssim 4$ GeV/c, followed by $R_{\rm HS} > 1$ for $p_T^{A,B} \gtrsim 5$ GeV/c. These trends reflect the competition between medium-induced modification and jet fragmentation and suggest that the latter dominates at $p_T^{A,B} \gtrsim 5$ GeV/c. The results shown in Fig. 1 indicate that, relative to $p+p$, the Au+Au yield is suppressed in the HR but is enhanced in the SR. We quantify this suppression/enhancement via $I_{\rm AA}$, the ratio of jet yield $Y_{\rm jet}$ between Au+Au and $p+p$ collisions over a $\Delta\phi$ region, W, $I_{\rm AA}^W = \int_{\Delta\phi\in W} d\Delta\phi Y_{\rm jet}^{\rm Au+Au} / \int_{\Delta\phi\in W} d\Delta\phi Y_{\rm jet}^{p+p}$.

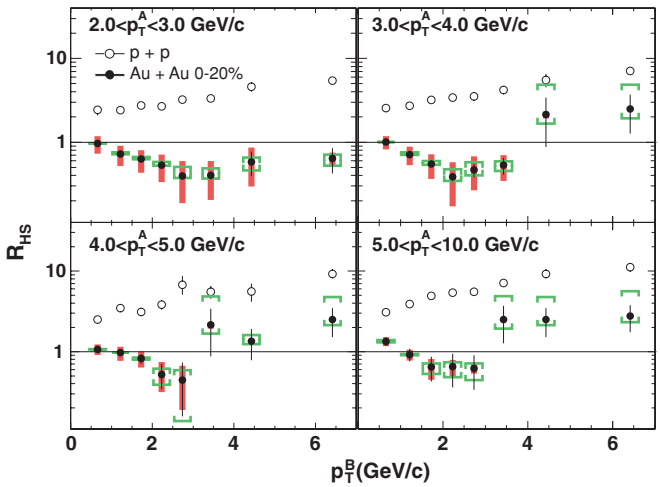

FIG. 2. (Color online) $R_{\rm HS}$ vs p_T^B for $p+p$ (open) and Au+Au (filled) collisions for four trigger selections. Because $R_{\rm HS}$ is purely hadron pair variable, the result is unchanged by swapping p_T^A and p_T^B. Shaded bars (brackets) represent p_T-correlated uncertainties due to elliptic flow (ZYAM procedure).

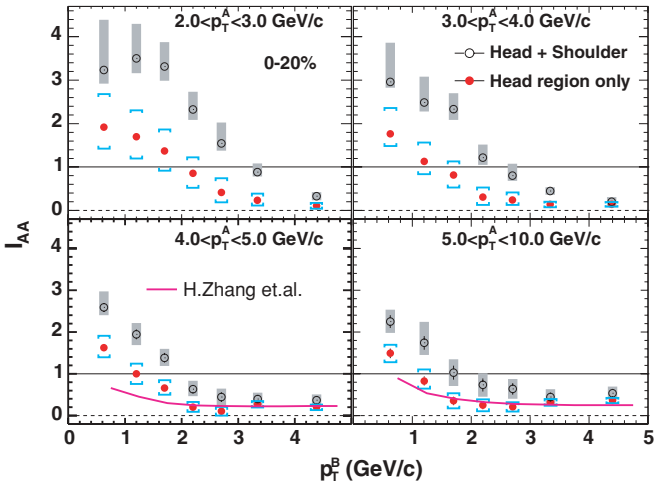

FIG. 3. (Color online) $I_{\rm AA}$ vs p_T^B for four trigger p_T bins in HR+SR ($|\Delta\phi - \pi| < \pi/2$) and HR ($|\Delta\phi - \pi| < \pi/6$). The systematic errors for the two regions, represented by shaded bars and brackets, respectively, include elliptic flow and ZYAM uncertainties and hence are strongly correlated. Grey bands around $I_{\rm AA} = 1$ represent 14% combined uncertainty on the single-particle efficiency in Au+Au and $p+p$. The thick curves are energy loss calculation from Ref. [21] for pairs in $|\Delta\phi - \pi| < 0.64$.

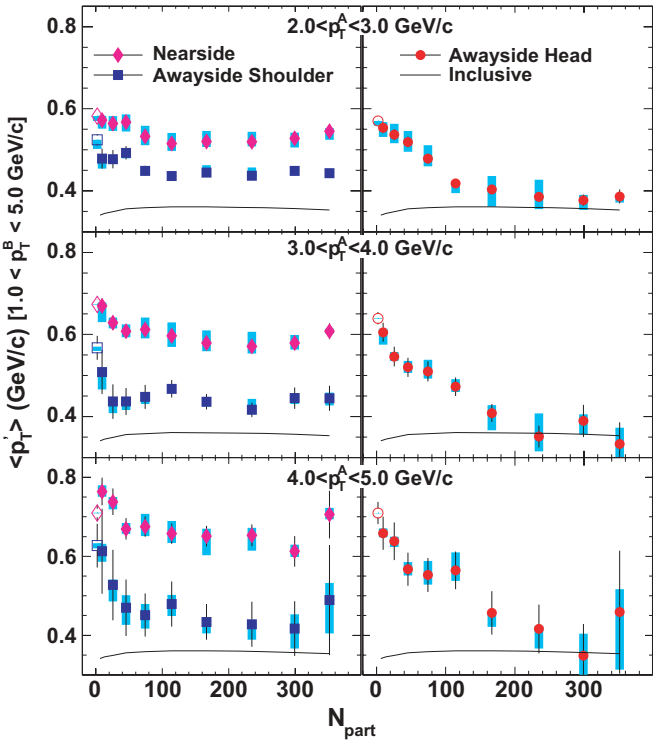

FIG. 4. (Color online) Truncated mean $\langle p'_T \rangle$ in $1 < p_T^B < 5$ GeV/c versus $N_{\rm part}$ for the near-side (diamonds), away-side shoulder (circles), and head (squares) regions for Au+Au (filled) and $p+p$ (open) for three trigger p_T bins. Solid curves represent values for inclusive charged hadrons (~0.36 GeV/c) [2]. Error bars represent the statistical errors. Shaded bars represent the sum of $N_{\rm part}$-correlated elliptic flow and ZYAM error.

Figure 3 shows $I_{\rm AA}$ as a function of p_T^B for the HR and the HR+SR, respectively, in four p_T^A bins. For triggers of $2 < p_{\rm T}^{\rm A} < 3$ GeV/c, $I_{\rm AA}$ for HR+SR exceeds one at low p_T^B, but falls and crosses one at ~3.5 GeV/c. A similar trend is observed for the higher p_T triggers, but the enhancement (at low p_T^B) is smaller and the suppression (at high p_T^B) is stronger. The $I_{\rm AA}$ values in HR are lower relative to HR+SR for all $p_T^{A,B}$. For the low p_T triggers, the suppression sets in around $1 \lesssim p_T^B \lesssim 3$ GeV/c, followed by a fall-off for $p_T^B \gtrsim 4$ GeV/c. For higher p_T triggers, a constant level of ~0.2–0.3 is observed above ~2 GeV/c. The suppression level is similar to the $R_{\rm AA}$ of inclusive hadrons [2] and agrees well with an energy loss model calculation [21] as indicated by the thick solid curves in Fig. 3. These results provide clear evidence for significant yield enhancement in the SR and suppression in the HR. The former reflects the dissipative processes that redistribute the energy lost in the medium, while the latter is consistent with jet quenching. However, we note that the $I_{\rm AA}$ values for the HR are upper limit estimates for the jet fragmentation component. This is because the HR yield includes possible contributions from the tails of the SR, as well as from bremsstrahlung gluon radiations [9].

To further contrast the HR and the SR, we focus on the p_T region of $1 < p_T^B < 5$ GeV/c, where the medium-induced component dominates the away-side. We characterize the inverse local slope of the partner yield in this p_T range via a truncated mean p_T, $\langle p'_T \rangle \equiv \langle p_T^B \rangle|_{1<p_T^B<5{\rm GeV}/c} - 1$ GeV/c. $\langle p'_T \rangle$ is calculated from the jet yields used to make $I_{\rm AA}$ in Fig. 3. Figure 4 shows the $\langle p'_T \rangle$ values for the HR, the SR, and a near-side region ($|\Delta\phi| < \pi/3$, NR) versus the number of participating nucleons, $N_{\rm part}$. The $\langle p'_T \rangle$ values for NR have a weak centrality dependence. Their overall levels for $N_{\rm part} > 100$ are 0.533 ± 0.024, 0.605 ± 0.032, and 0.698 ± 0.040 GeV/c for the p_T^A ranges 2–3, 3–4, and 4–5 GeV/c, respectively [22]. This is consistent with the dominance of jet fragmentation on the near-side, i.e., a harder spectrum for partner hadrons is expected for higher p_T trigger hadrons.

A very weak centrality dependence is observed for the SR for $N_{\rm part} \gtrsim 100$. In this case, the values for $\langle p'_T \rangle$ are lower (≈0.45 GeV/c) and do not depend on p_T^A. They are, however, larger than the values for inclusive charged hadrons [2]. The relatively sharp increase in $\langle p'_T \rangle$ for $N_{\rm part} \lesssim 100$ may reflect a significant jet fragmentation contribution in peripheral collisions. In contrast, the $\langle p'_T \rangle$ values for the HR show a gradual decrease with $N_{\rm part}$, starting close to that for the near-side jet, and approach the value for the inclusive spectrum for $N_{\rm part} \gtrsim 150$.

The different patterns observed for the yields in the HR and SR suggest a different origin for these yields. The suppression of the HR yield and the softening of its spectrum are consistent with a depletion of yield due to jet quenching. Further evidence is given by high p_T pairs, for which the HR yield agrees with energy loss calculations [21] and the HR shape becomes jet like. This suggests that these pairs come mainly from the fragmentation of partons that suffer small energy loss due to tangential or punch-through jet emissions. By contrast, the enhancement of the SR yield reflects a remnant of the lost energy from quenched jets. This enhancement is limited to

$p_T^{A,B} \lesssim 4$ GeV/c, the same p_T region where the soft processes such as hydrodynamical flow and recombination are important. The spectra slope of the SR is almost independent of p_T^A and centrality (for $N_{\rm part} \gtrsim 100$), reflecting an intrinsic property of the response of the medium to the energetic jets. These observations provide separate constraints on geometrical bias at high p_T [19–21] and on the energy transport at low p_T [7–11,23]. However, a model framework including both jet quenching and medium response, which can describe the full p_T evolution of the away-side jet shape and yield, is required to understand the parton-medium interactions.

In conclusion, we have observed strong medium modification of away-side shapes and yields for jet-induced pairs in Au+Au collisions at $\sqrt{s_{\rm NN}} = 200$ GeV. The detailed dependence of these results on p_T and centrality gives strong evidence for two distinct contributions from the regions of $\Delta\phi \sim \pi$ and $\Delta\phi \sim \pi \pm 1.1$. The former shows a strong yield suppression, with a level consistent with a jet quenching calculation at high p_T. The latter exhibits p_T and centrality independent shape and mean p_T, possibly reflecting an intrinsic property of the medium response to energetic jets.

We thank the staff of the Collider-Accelerator and Physics Departments at BNL for their vital contributions. We acknowledge support from the Office of Nuclear Physics in the DOE Office of Science and NSF (USA); MEXT and JSPS (Japan); CNPq and FAPESP (Brazil); NSFC (China); MSMT (Czech Republic); IN2P3/CNRS and CEA (France); BMBF, DAAD, and AvH (Germany); OTKA (Hungary); DAE (India); ISF (Israel); KRF and KOSEF (Korea); MES, RAS, and FAAE (Russia); VR and KAW (Sweden); USA CRDF for the FSU; US-Hungarian NSFOTKA-MTA; and US-Israel BSF.

[1] M. Gyulassy, I. Vitev, X. N. Wang, and B. W. Zhang, in *Quark Gluon Plasma*, edited by R. C.Hwa and X. N. Wang (World Scientific, Singapore, 2003), pp. 123–191; A. Kovner and U. A. Wiedemann, in *Quark Gluon Plasma*, edited by R. C. Hwa and X. N. Wang (World Scientific, Singapore, 2003), pp. 192–248.
[2] S. S. Adler *et al.*, Phys. Rev. C **69**, 034910 (2004).
[3] J. Adams *et al.*, Phys. Rev. Lett. **97**, 162301 (2006).
[4] S. S. Adler *et al.*, Phys. Rev. Lett. **97**, 052301 (2006).
[5] A. Adare *et al.*, Phys. Rev. Lett. **98**, 232302 (2007).
[6] J. Adams *et al.*, Phys. Rev. Lett. **95**, 152301 (2005).
[7] C. B. Chiu and R. C. Hwa, Phys. Rev. C **74**, 064909 (2006).
[8] N. Armesto, C. A. Salgado, and U. A. Wiedemann, Phys. Rev. Lett. **93**, 242301 (2004).
[9] I. Vitev, Phys. Lett. **B630**, 78 (2005); A. D. Polosa and C. A. Salgado, Phys. Rev. C **75**, 041901(R) (2007).
[10] I. M. Dremin, JETP Lett. **30**, 140 (1979); V. Koch, A. Majumder, and X. N. Wang, Phys. Rev. Lett. **96**, 172302 (2006).
[11] J. Casalderrey-Solana, E. V. Shuryak, and D. Teaney, J. Phys. Conf. Ser. **27**, 22 (2005); arXiv:hep-ph/0602183.
[12] K. Adcox *et al.*, Nucl. Instrum. Methods A **499**, 469 (2003).
[13] A. Adare *et al.*, Phys. Rev. Lett. **97**, 252002 (2006).
[14] S. S. Adler *et al.*, Phys. Rev. C **73**, 054903 (2006).
[15] S. S. Adler *et al.*, Phys. Rev. Lett. **95**, 202001 (2005).
[16] S. S. Adler *et al.*, Phys. Rev. Lett. **91**, 182301 (2003).
[17] J. Jia (PHENIX Collaboration), Nucl. Phys. **A783**, 501 (2007).
[18] N. N. Ajitanand *et al.*, Phys. Rev. C **72**, 011902(R) (2005).
[19] T. Renk and K. J. Eskola, Phys. Rev. C **75**, 054910 (2007).
[20] C. Loizides, Eur. Phys. J. C **49**, 339 (2007).
[21] H. Zhang, J. F. Owens, E. Wang, and X. N. Wang, Phys. Rev. Lett. **98**, 212301 (2007), and additional calculations from H. Zhang.
[22] Values at $N_{\rm part} > 100$ are slightly lower than in $p+p$, possibly due to a contribution from a near-side "ridge" [6] in PHENIX η acceptance.
[23] T. Renk and J. Ruppert, Phys. Rev. C **73**, 011901(R) (2006).